Physics Letters B 817 (2021) 136286

Contents lists available at ScienceDirect

Physics Letters B

www.elsevier.com/locate/physletb

Triple enhancement of quasi-SU(3) quadrupole collectivity in Strontium-Zirconium $N \approx Z$ isotopes

K. Kaneko [a], N. Shimizu [b], T. Mizusaki [c], Y. Sun [d,*]

[a] Department of Physics, Kyushu Sangyo University, Fukuoka 813-8503, Japan
[b] Center for Nuclear Study, The University of Tokyo, 7-3-1 Hongo Bunkyo, Tokyo 113-0033, Japan
[c] Institute of Natural Sciences, Senshu University, Tokyo 101-8425, Japan
[d] School of Physics and Astronomy, Shanghai Jiao Tong University, Shanghai 200240, China

ARTICLE INFO

Article history:
Received 26 February 2021
Received in revised form 5 April 2021
Accepted 8 April 2021
Available online 14 April 2021
Editor: J.-P. Blaizot

ABSTRACT

It is notable that along the $N = Z$ line in the nuclear chart, extremely large collectivity emerges suddenly in the mass-80 region. By applying the Monte Carlo shell model (MCSM) and the Hartree-Fock-Bogolyubov plus generator coordinate method (HFB+gcm), we study this problem to find the origin. On the basis that both calculations reproduce the experimental data of the $N \approx Z$ nuclei with $A = 64 \sim 88$, we identify the backbone from full shell-model calculations that can explain the strong prolate deformation. We find that inclusion of the $2d_{5/2}$ orbit in the model space to cooperate with $1g_{9/2}$ is the key ingredient to describe the rapid increase of collectivity from ^{70}Se to ^{76}Sr and to produce the observed large $B(E2)$ values in ^{76}Sr, ^{78}Sr and ^{80}Zr. The quadrupole-quadrupole (QQ) interaction acting between the quasi-SU(3) partner orbits, $1g_{9/2} - 2d_{5/2}$, is the driving force that changes the nuclear shape from oblate- to prolate-deformed. We further suggest that the quasi-SU(3) effect is particularly amplified in the $N \approx Z$ nuclei because these are the unique examples where quasi-SU(3) partner orbits can be formed, like the nuclear pairing, simultaneously in three different types: neutron-neutron (n-n), proton-proton (p-p), and neutron-proton (n-p), which respectively interact through the n-n, p-p, and n-p components of the QQ force to enhance the quadrupole collectivity coherently.

Nuclei along the $N = Z$ line exhibit unique properties. In the self-conjugate nuclei having equal proton and neutron numbers, the valence protons and neutrons occupy the same single-particle orbits, and thus have the largest spatial overlaps. The two types of fermions, neutrons and protons, can couple to form isovector $T = 1$ triplet pairs (with antiparallel spins) and isoscalar $T = 0$ singlet pair (with parallel spins). Moreover, those $N = Z$ nuclei with equal even-numbers of neutrons and protons are compositions of α particles, and have extra stability. The ^{64}Ge, ^{68}Se, ^{72}Kr, ^{76}Sr, and ^{80}Zr nuclei are known as waiting-points [1] in the rapid proton-capture process (rp-process), showing large local abundances in nucleosynthesis.

Since the pioneering work of Lister et al. [2,3], it has become to know that in a small mass region near $N = Z = 40$, some neutron-deficient isotopes have outstandingly large prolate-deformation. With the help of later experiments, one has established the full image of ground-state shape-evolution along the $N = Z$ line, varying from triaxial shape for ^{64}Ge [4], via oblate for ^{68}Se [5] and ^{72}Kr [6–8], to strongly prolate for ^{76}Sr [9–11] and ^{80}Zr [11,12]. It is especially noticed that the onset of large quadrupole collectivity with prolate deformation occurs very suddenly near $N = Z = 36$, which is suggested as an example of shape phase transition [13].

The reduced electric quadrupole transition probability, $B(E2, 2_1^+ \to 0_1^+)$ (hereafter denoted as $B(E2\downarrow)$), and the energy of the first excited 2_1^+ state, $E_x(2_1^+)$ are commonly used as measures of quadrupole collectivity. In a recent experiment [11], lifetimes of the first excited 2^+ states in ^{76}Sr, ^{78}Y, and ^{80}Zr have been measured. The extracted $B(E2\downarrow)$ yield new information on where in the mass region the collectivity is maximized. The data show that the maximum centers on ^{76}Sr with $B(E2\downarrow)$ = 2390(240) (e^2fm^4), followed by 1910(180) in ^{80}Zr and 1840(100) in the $N = Z + 2$ nucleus ^{78}Sr. The experiment has also observed $B(E2\downarrow) = 1200^{+180}_{-250}$ in the odd-odd $N = Z$ nucleus ^{78}Y, which is considerably smaller than those of the neighboring even-even nuclei, raising a question if in this mass region, an odd-odd vs. even-even staggering in $B(E2)$ is general. These data, together with the previous measurements, are summarized in Fig. 1, where one can clearly see the drastic changes in $B(E2\downarrow)$ and E_x with mass number A. Especially, the rapid increase in $B(E2\downarrow)$ is evident when the mass

* Corresponding author.
E-mail address: sunyang@sjtu.edu.cn (Y. Sun).

https://doi.org/10.1016/j.physletb.2021.136286

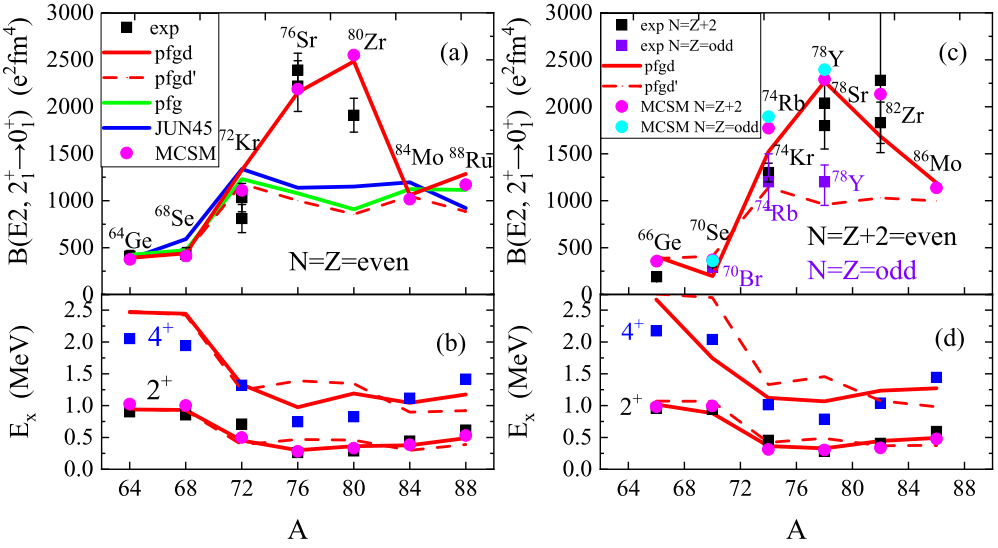

Fig. 1. HFB+gcm and MCSM calculations compared with experimental data. (a) $B(E2\downarrow)$, and (b) first 2^+ and 4^+ energy for $N=Z=$ even nuclei, (c) $B(E2\downarrow)$ for $N=Z+2=$ even and $N=Z=$ odd nuclei, and (d) first 2^+ and 4^+ energy for $N=Z+2=$ even nuclei. Data are shown by black (violet) squares for even-even (odd-odd) nuclei and taken from Refs. [2–11,14–16].

number changes from $A=72$ to $A=76$, and the $B(E2\downarrow)$ peaks at the $N=Z$ and the neighboring $N=Z+2$ Strontium-Zirconium isotopes.

What is the origin for the rapid onset of large prolate deformation at $N=Z=36$ and the emergence of outstandingly-large collectivity only in a narrow region centering on $N=Z=40$? Early calculations by the deformed single-particle mean-field models (see, for example, Ref. [17]) suggested contribution from the $1g_{9/2}$ intruder orbit. Later studies by the shell model Monte Carlo [18] and the large-scale shell model [13] found that the $2d_{5/2}$ orbit has a cooperative effect for enhancing the $1g_{9/2}$ contribution. The calculations using EXCITED VAMPIR approximation [19] and Projected Shell Model [20] also included $2d_{5/2}$ in the model space. To understand the cooperation effect of $1g_{9/2}$ and $2d_{5/2}$, Zuker et al. put forward an idea by suggesting the quasi-SU(3) scheme [21] as the backbone of a full shell-model description for large prolate deformation. The essence of this scheme is that enhanced collectivity is produced by quasi-SU(3) partner orbits, which are coupled by the quadrupole force and central field in the subspace with $\Delta j=2$ orbits.

Let us mention an example from the lighter mass region where conventional shell models can work. Large collectivity was reported in the neutron-rich nucleus ^{64}Fe with $N=38$ [22], where a jump of $B(E2\downarrow)$ from 214(26) e^2fm^4 in ^{62}Fe to 470^{+210}_{-110} e^2fm^4 in ^{64}Fe was observed. In the theoretical explanation, Lenzi et al. showed [23] that, while the contribution of $1g_{9/2}$ orbit is important, the inclusion of the $2d_{5/2}$ orbit in the shell model is needed to explain the sudden increase of the $B(E2)$ value. The $1g_{9/2}$ and $2d_{5/2}$ orbits are described as a partner in the quasi-SU(3) scheme [21,24], and play a joint role in producing large collectivity in the neutron-rich Cr and Fe nuclei near $N=40$. The neutron $N=40$ subshell gap is effectively reduced if the proton number is less than $Z=28$ (such as Fe isotopes), and the neutron excitations into $1g_{9/2}$-$2d_{5/2}$ largely increase $B(E2)$ at $N=40$.

With protons added to ^{68}Ni, even more enhanced collectivity would emerge when the proton number also approaches 40. Data show that, across a few mass units, $B(E2)$ jumps drastically from 332(37) e^2fm^4 in ^{70}Se [15] to 2390(240) e^2fm^4 in ^{76}Sr [11], increasing by more than seven times. The enhancement ratio is much larger than that in ^{64}Fe (about two times). We may speculate that the huge difference in enhancement ratio is due to the particular case in the $N=Z=40$ region where the quasi-SU(3) partner $(1g_{9/2},\ 2d_{5/2})$ is formed from both protons and neutrons, which cooperatively enhance the $E2$ collectivity.

For well-deformed $A\sim 80$ nuclei, the conventional shell-model based on the Lanczos diagonalization is out of applicability due to dimension explosion. To study the current problem, one needs to apply advanced many-body techniques to make calculations feasible [25]. Regardless of details in different models, the guideline for such calculations may include the following steps. One first identifies relevant basis states by using either Hartree-Fock-Bogolyubov (HFB) or Monte Carlo methods. As these states are generally deformed quasiparticle states that do not conserve angular momentum and particles number, one then restores the broken symmetries by the projection technique. The projected states serve as building blocks for constructing many-body configurations in which a chosen Hamiltonian is finally diagonalized. The Projected Shell Model [26,27], the Monte Carlo Shell Model (MCSM) [28,29] implemented in Ref. [30], the HFB plus generator coordinate method (HFB+gcm) with the largest computer code written recently [31], and the methods developed by the Madrid group [32,33], fall into this category.

In this Letter, we apply MCSM and HFB+gcm, employing the PMMU Hamiltonian proposed in Ref. [34] for the model space of $(2p_{3/2}, 1f_{5/2}, 2p_{1/2}, 1g_{9/2}, 2d_{5/2})$ (referred hereafter to as $pfgd$). Previously with the smaller model space $(2p_{3/2}, 1f_{5/2}, 2p_{1/2}, 1g_{9/2})$ without $2d_{5/2}$ (referred to as pfg), we demonstrated [35] that the PMMU Hamiltonian works well for describing nuclear properties such as binding energies, energy spectra, and electromagnetic transitions in the lower part of the pfg-shell nuclei from Ni to Se isotopes.

It may be advantageous for studying the current problem by using the Hamiltonian with separable forces, because one can easily identify the essential interactions and orbits from large numerical calculations. For justification of using the separable forces, Dufour and Zuker showed [36] that any practical effective interactions for nuclear structure calculations are dominated by the pairing plus quadrupole-quadrupole ($P+QQ$) terms with monopole interaction. Employing the monopole interaction constructed from the monopole-based universal force [37], we have successfully applied the PMMU interaction in the pf [38] and the pfg [35] model spaces. The PMMU interaction has recently been further applied in the HFB+gcm method for Sn, Te, Xe, Ba, Ce, Nd, and Sm isotopes [39], where we showed that the quasi-SU(3) partner $(1h_{11/2},2f_{7/2})$

plays an important role in the explanation of large collectivity in the mass $A = 130$ region.

The PMMU Hamiltonian contains four basic terms [35,38]

$$H = H_0 + V_P + V_{QQ} + V_m^{MU}. \quad (1)$$

H_0 and V_P are the single-particle Hamiltonian and (monopole and quadrupole) pairing interaction, respectively. The third term in (1) is the QQ interaction

$$V_{QQ} = -\frac{1}{2}\chi_2 \sum_{M,a,b,c,d} Q^\dagger_{2M}(a,b)\, Q_{2M}(c,d) + h.c. \quad (2)$$

Although not explicitly expressed, Eq. (2) is of the vector type that includes, in addition to the n-n and p-p terms, also the n-p term. The letters a, b, c, and d denote individual orbits, excluding double counting. The present calculation employs the same single-particle energies and force strengths as in the pfg model space [35]. The last term is the monopole interaction V_m^{MU} constructed from the monopole-based universal force [37]. The monopole interaction matrix elements between the $2d_{5/2}$ orbit and the pfg shell are constructed from the monopole-based universal force [37]. The monopole Hamiltonian and the single-particle energy for $2d_{5/2}$ are slightly modified from those in Refs. [35,38] so as to fit precisely the experimental data. All the monopole matrix elements are scaled with a factor $(58/A)^{0.3}$ in the calculation. The spurious center-of-mass motion is removed by the Lawson method [40].

We present the calculated $B(E2\downarrow)$ values in the $pfgd$ model space for the $N = Z =$ even nuclei in Fig. 1(a) and $N = Z + 2 =$ even and $N = Z =$ odd nuclei in Fig. 1(c), from $A = 64$ to $A = 88$. It is well known that for shell-model calculations, the choice of effective charges depends on the employed model space and the way of nucleon excitations. For the present calculation, the effective charges are chosen as $e_p = 1.9e$ and $e_n = 0.5e$ so as to fit the experimental $B(E2)$ values, while the standard values $e_p = 1.5e$ and $e_n = 0.5e$ cannot reproduce the observed data. It is noticed that overall, the two theoretical results, HFB+gcm and MCSM, remarkably agree with each other. To compare them with data, both theories reproduce the trend of evolution in $B(E2\downarrow)$ correctly, with the odd-odd nucleus ^{78}Y as an exception (we shall comment on this nucleus later). In Fig. 1 (b) and (d), the energy levels for the first excited 2^+_1 and 4^+_1 states are compared for $N = Z =$ even and $N = Z + 2 =$ even nuclei, respectively. The two theoretical calculations in the $pfgd$ model space are overall in good agreement with the experimental 2^+_1 states, while for 4^+_1 states, correct variation trend as A varies is obtained.

To emphasize the effect from the $2d_{5/2}$ orbit, we carry out calculations using the PMMU [35] and JUN45 [41] interactions in the pfg model space. The effective charges are taken as $e_p = 1.5e$ and $e_n = 1.1e$ for both calculations. Without $2d_{5/2}$, the calculated $B(E2\downarrow)$ values drastically drop for ^{76}Sr and ^{80}Zr in Fig. 1(a), and for ^{78}Sr and ^{82}Zr (not shown in Fig. 1(b)). For all other isotopes, the results of the $pfgd$ and pfg model spaces are essentially the same. This drop is a clear evidence that the $2d_{5/2}$ orbit plays a decisive role in generating large collectivity only for ^{76}Sr, ^{78}Sr, ^{80}Zr, and ^{82}Zr.

In the quasi-SU(3) scheme [21,24], the partner orbits with $\Delta j = 2$, $(1g_{9/2}, 2d_{5/2})$ in our case, are coupled by the QQ force to create large quadrupole collectivity. To further study the quasi-SU(3) effect, the relevant part in the QQ interaction

$$V^{gd}_{QQ} = -\frac{1}{2}\chi_2 \sum_{M,c,d} Q^\dagger_{2M}(1g_{9/2}, 2d_{5/2})\, Q_{2M}(c,d) + h.c. \quad (3)$$

is extracted from Eq. (2). The calculation with the remaining QQ part in PMMU (labeled as $pfgd'$) is shown by broken red lines in Fig. 1 (a)-(d). It can be clearly seen that the so-calculated $B(E2\downarrow)$ are almost the same as the PMMU ones in the pfg space. Thus without the contribution of V^{gd}_{QQ} in Eq. (3), the large enhancement in quadrupole collectivity, obtained with the $pfgd$ space for ^{76}Sr, ^{78}Sr, ^{80}Zr, and ^{82}Zr, disappears. This result confirms unambiguously the contribution of the quasi-SU(3) effect in enhancing quadrupole collectivity in the $N = Z = 40$ mass region. For energy levels, the effect is weaker. As Fig. 1(b) and 1(d) show, without V^{gd}_{QQ}, the changes in the 2^+ and 4^+ state energy are not very much.

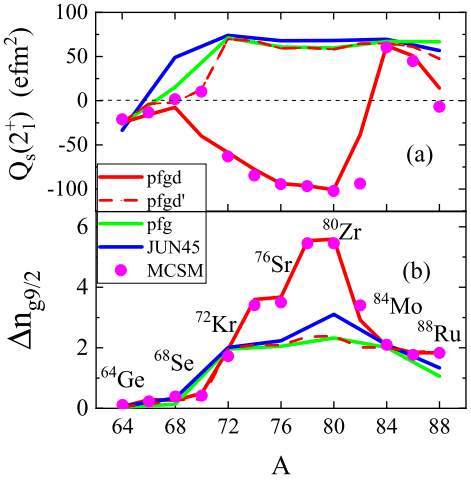

Fig. 2. Calculated spectroscopic quadrupole moments and extra $1g_{9/2}$ occupancies for $N = Z, Z + 2$ nuclei.

In Fig. 2 (a), calculated spectroscopic quadrupole moments (Q_s) by HFB+gcm and MCSM are shown for first excited 2^+ states of even-even $N = Z, Z+2$ nuclei. For comparison, results from PMMU and JUN45 calculations in the pfg space are also presented. For all the nuclei of interest, the results in the pfg space, as well as those from HFB+gcm in the $pfgd'$ space, show either very small or positive Q_s, corresponding to near-spherical or oblate deformation. On the other hand, the HFB+gcm calculation in the $pfgd$ space shows similar results for the mass number $A = 64, 66, 68$, and 84, 86, 88, but for $A = 74$ to 82, the obtained Q_s are large and negative, indicating that these nuclei are strongly prolate-deformed. For $A = 70$, the HFB+gcm (MCSM) calculation indicates moderate value of negative (positive) Q_s. The $A = 72$ nucleus, ^{72}Kr, is commonly considered to have prolate-oblate shape-coexistence near the ground state; both of our calculations suggest a prolate deformation for the first excited 2^+ state.

Large prolate deformation in these nuclei is known [42] and usually interpreted as due to the polarization of the $1g_{9/2}$ orbit [17]. We can understand the problem from a different aspect by looking at the occupations of the intruder $1g_{9/2}$ orbit. Fig. 2(b) shows the extra occupancy number, $\Delta n_{g9/2}$, for protons, which is the difference between $n_{g9/2}$ obtained with configuration mixing and the one corresponding to the normal filling. One sees that $\Delta n_{g9/2}$ is very small for ^{64}Ge and ^{68}Se, becomes ~ 2 for ^{72}Kr, and then drastically increases to ~ 4 in ^{76}Sr, and to ~ 6 in ^{80}Zr. The results from the HFB+gcm in $pfgd$ and MCSM are remarkably similar. The variation in extra $n_{g9/2}$ occupancies has a one-to-one correspondence with the changes in $B(E2\downarrow)$ in Fig. 1(a) and Q_s in Fig. 2(a). In contrast, $\Delta n_{g9/2}$ from the PMMU and JUN45 calculations in the pfg space gets ~ 2 for ^{76}Sr and ^{80}Zr, consistent with the results for ^{64}Cr and ^{64}Fe [18].

In Table 1, the $1g_{9/2}$ and $2d_{5/2}$ occupation numbers (for protons or neutrons) are shown for the $N = Z$ nuclei with the $pfgd$ and $pfgd'$ calculations. It is notable that due to the V^{gd}_{QQ} force, the $1g_{9/2}$ occupancies for ^{76}Sr and ^{80}Zr are greatly enhanced together with the $2d_{5/2}$ occupancy in the $pfgd$ calculation. The other

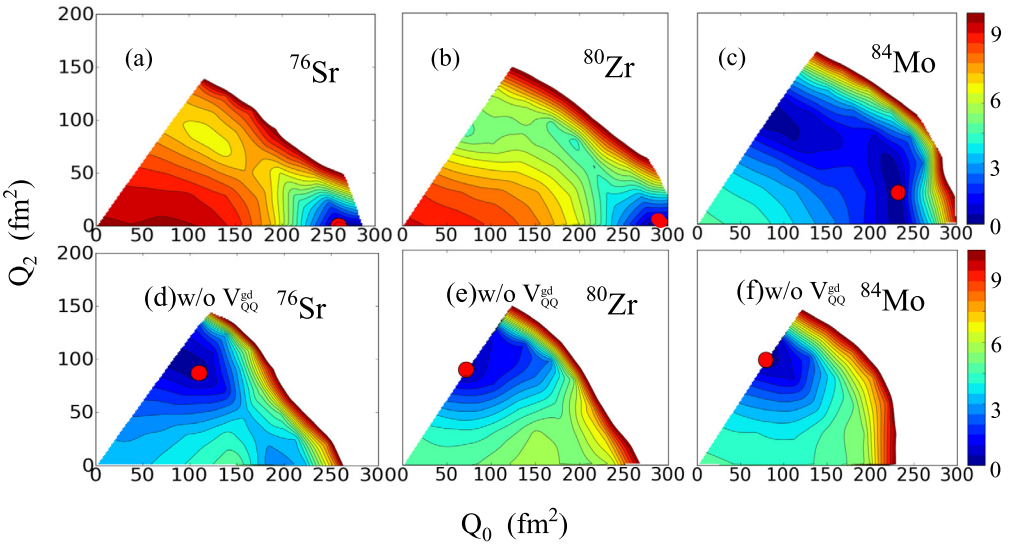

Fig. 3. Potential energy surface (PES) for the ground-state of ^{76}Sr, ^{80}Zr, and ^{84}Mo in HFB calculations. The upper (lower) graphs show PES with (without) V^{gd}_{QQ}. Red dots indicate the local minima.

Table 1
Occupation numbers of the $1g_{9/2}$ and $2d_{5/2}$ orbits of the ground state for the $pfgd$ and $pfgd'$ calculations using the HFB+gcm.

	cal($pfgd$)		cal($pfgd'$)	
	$1g_{9/2}$	$2d_{5/2}$	$1g_{9/2}$	$2d_{5/2}$
^{64}Ge	0.057	0.004	0.052	0.003
^{68}Se	0.253	0.024	0.280	0.031
^{72}Kr	1.949	0.073	1.969	0.002
^{76}Sr	3.597	0.394	2.084	0.001
^{80}Zr	5.577	0.367	2.389	0.002
^{84}Mo	4.060	0.031	4.005	0.003

interactions including the monopole force do not produce such a pronounced occupation enhancement. For ^{84}Mo the Pauli blocking effect prohibits more excitations to $1g_{9/2}$, as it is already occupied by four protons (neutrons). Therefore, the $1g_{9/2}$ occupations in ^{84}Mo are similar for $pfgd$ and $pfgd'$ calculations.

The influence of V^{gd}_{QQ} on shapes can be visualized in plots of potential energy surface (PES). Fig. 3 shows PES from the HFB calculation for ^{76}Sr, ^{80}Zr, and ^{84}Mo. The upper (lower) graphs display the PES in $pfgd$ calculations with V^{gd}_{QQ} ($pfgd'$ without V^{gd}_{QQ}). By comparing the upper and lower graphs, we conclude that V^{gd}_{QQ} can influence deformed shapes qualitatively. For ^{76}Sr and ^{80}Zr, V^{gd}_{QQ} drives the shape from oblate to strongly prolate, consistent with the large $B(E2\downarrow)$ observed in ^{76}Sr [10] and ^{80}Zr [11]. For ^{84}Mo, there are several previous predictions for its ground-state shape: prolate- and triaxial-deformed [12], prolate-oblate shape coexistence [19], oblate-deformed [43], and soft axial-symmetric [44]. Our calculated PES suggests that V^{gd}_{QQ} changes the ^{84}Mo shape from oblate to an extremely-soft energy surface that slightly favors prolate.

A remaining question is how to understand the observed $B(E2\downarrow)$ in the $N=Z=39$ nucleus ^{78}Y [11], which was reportedly much smaller than those of the neighboring $N=Z=$ even ^{76}Sr and ^{80}Zr, and also smaller than that of its isobaric analogue state (IAS) of the $N=Z+2$ nucleus ^{78}Sr (see Fig. 1(c)). We have performed systematic calculations for the odd-odd $N=Z$ nuclei ^{70}Br, ^{74}Rb, and ^{78}Y, and the even-even $N=Z+2$ nuclei ^{70}Se, ^{74}Kr, and ^{78}Sr. As shown in Fig. 1 (c), clear deviation with experimental $B(E2\downarrow)$ occurs only for ^{78}Y. The difference in $B(E2\downarrow)$ between ^{78}Y and the IAS in ^{78}Sr may suggest large isospin symmetry breaking (ISB). However, another ISB indicator, i.e., the Coulomb energy difference (CED), is found small for the low-lying states in mass $A=78$ [45]. Moreover, the calculated $B(E2\downarrow)$ for ^{70}Br and ^{70}Se, and ^{74}Rb and ^{74}Kr, show respectively similar values, which are consistent with the experimental observation. Thus, interpretation of the observed smaller $B(E2\downarrow)$ in ^{78}Y [11] remains an open question at present.

The density functional theory (DFT) calculation including the isovector ($T=1$) pairing cannot explain the observed low $B(E2\downarrow)$ value in ^{78}Y [11]. The authors speculated that the inclusion of the isoscalar ($T=0$) np pairing would be a solution. Over the years, many theoretical and experimental works have been devoted to finding evidence for the $T=0$ np pairing. It was predicted [34] for the $N=Z$ nucleus ^{88}Ru that the $T=0$ np pairing interaction plays an important role in enhancing the high-spin collectivity, leading to delayed band-crossing. The prediction was later confirmed experimentally [46].

To discuss the contributions from $T=0$ and $T=1$ pairing of the V^{gd}_{QQ} interaction in the present $pfgd$ calculation, the multipole form of V^{gd}_{QQ} in Eq. (3) is transformed into terms of the pairing form with the isospin $T=0$ and 1 [34,36]. In Fig. 4, the calculations without the $T=0$ or $T=1$ term are compared. Fig. 4(a) shows that the $B(E2)$ values in the mass $A=76-80$ are largely reduced by neglecting the $T=1$ pairing term, while the $T=0$ term of V^{gd}_{QQ} does not affect the result entirely. This thus concludes that the $T=1$ pairing is more important for large collectivity. In Fig. 4(b), spectroscopic quadrupole moment Q_s indicates that the deformed shape changes from oblate to prolate in $A=74-80$ are also due to the V^{gd}_{QQ} with $T=1$. The above results are consistent with the enhancement of extra $1g_{9/2}$ occupancy in $A=74-80$ due to the $T=1$ pairing (see Fig. 4(c)). Thus, our results through the study of the V^{gd}_{QQ} interaction suggest the importance of the $T=1$ pairing term for the large collectivity around $A=80$, while the influence of the $T=0$ pairing cannot be found in the low-lying states.

To summarize, experiments have confirmed the rapid onset of large quadrupole collectivity along the $N=Z$ line and the maximal prolate deformation in the $A=80$ Strontium-Zirconium region. The origin is however not very clear. We have investigated this problem by performing HFB+gcm and MCSM calculations in the $fpgd$ model space. We have found that the quasi-SU(3) coupling scheme [21,24], applied by Lenzi et al. [23] to explain the

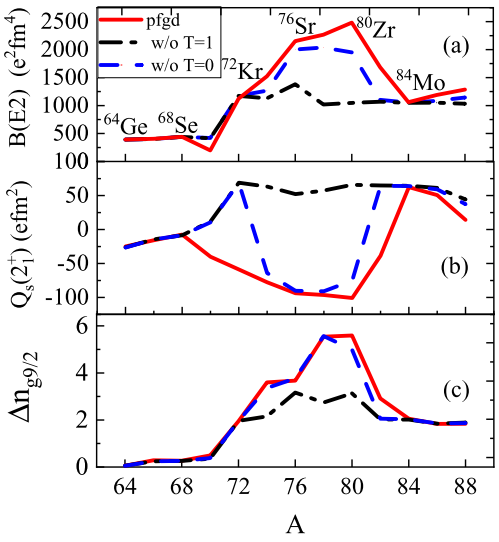

Fig. 4. $B(E2)$ values, spectroscopic quadrupole moments, and extra $1g_{9/2}$ occupancies for neutrons in the $pfgd$ calculation without the $T=1$ or $T=0$ term in V_{QQ}^{gd}.

enhanced collectivity in ^{64}Fe, is the backbone among various configurations that enhances the $E2$ collectivity and drives shapes to prolate deformation. The occupancy of the quasi-SU(3) partner orbits $1g_{9/2}$ and $2d_{5/2}$ becomes the largest for ^{76}Sr and ^{80}Zr, where unusually-large $B(E2)$ collectivity is found.

A similar conclusion to explain the large $B(E2)$ values in ^{124,126}Ce, ^{130,132}Nd and ^{134}Sm of the $A=130$ mass region has been obtained, where the quasi-SU(3) partner $(1h_{11/2},2f_{7/2})$ plays a role [39]. Compare to the examples for the $A=60$ [23] and $A=130$ [39] mass regions, the current work for the $A=80$ region has presented an outstanding example with the enhancement rate much larger than all other known cases. We have found that for $N\approx Z$ nuclei where neutrons and protons occupy the same orbits, the quasi-SU(3) coupling scheme is realized with n-n, p-p, and n-p types simultaneously. This is analogous to the pairing mechanism with three kinds of Cooper pairs specifically in nuclear physics. The above enhancement mechanism is supported by qualitative estimates by using different measures for quadrupole collectivity. It is easy to show that by using the same effective charges, the squared ratio of mass quadrupole moments between ^{76}Sr and ^{64}Cr is 3.06, while that of intrinsic (electric) quadrupole moments (with the value for ^{76}Sr from our calculation and that for ^{64}Cr from Ref. [23]) is 3.31, both of which are close to three times in enhancement. The present example thus represents rare cases in the nuclear chart, if not the unique one, of triple enhancement in quadrupole collectivity through the n-n, p-p, and n-p types of quasi-SU(3) coupling.

This work was partially supported by the National Key Program for S&T Research and Development of China (No. 2016YFA0400501) and by the National Natural Science Foundation of China (No. U1932206). The numerical calculation was performed mainly on the Oakforest-PACS supercomputer for Multidisciplinary Computational Sciences Project of Tsukuba University (xg18i035). NS acknowledges the supports by Program for Promoting Researches on the Supercomputer "Fugaku" (Simulation for basic science: from fundamental laws of particles to creation of nuclei) and the KAKENHI grant (17K05433).

Declaration of competing interest

The authors declare that they have no known competing financial interests or personal relationships that could have appeared to influence the work reported in this paper.

References

[1] H. Schatz, et al., Phys. Rep. 294 (1998) 167.
[2] C.J. Lister, et al., Phys. Rev. Lett. 49 (1982) 308.
[3] C.J. Lister, et al., Phys. Rev. Lett. 59 (1987) 1270.
[4] K. Starosta, et al., Phys. Rev. Lett. 99 (2007) 042503.
[5] A. Obertelli, et al., Phys. Rev. C 80 (2009) 031304(R).
[6] E. Bouchez, et al., Phys. Rev. Lett. 90 (2003) 082502.
[7] A. Gade, et al., Phys. Rev. Lett. 95 (2005) 022502.
[8] H. Iwasaki, et al., Phys. Rev. Lett. 112 (2014) 142502.
[9] E. Nacher, et al., Phys. Rev. Lett. 92 (2004) 232501.
[10] A. Lemasson, et al., Phys. Rev. C 85 (2012) 041303(R).
[11] R.D.O. Llewellyn, et al., Phys. Rev. Lett. 124 (2020) 152501.
[12] S.J. Zheng, et al., Phys. Rev. C 90 (2014) 064309.
[13] M. Hasegawa, K. Kaneko, T. Mizusaki, Y. Sun, Phys. Lett. B 656 (2007) 51.
[14] Data extracted using the NNDC World Wide Web site from the ENDSF data base.
[15] A.J. Nicols, et al., Phys. Lett. B 733 (2014) 52.
[16] C. Morse, et al., Phys. Lett. B 787 (2018) 198.
[17] W. Nazarewicz, J. Dudek, R. Bengtsson, T. Bengtsson, I. Ragnarsson, Nucl. Phys. A 435 (1985) 397.
[18] K. Langanke, D.J. Dean, W. Nazarewicz, Nucl. Phys. A 728 (2003) 109.
[19] A. Petrovici, K.W. Schmid, A. Faessler, Nucl. Phys. A 605 (1996) 290.
[20] Y. Sun, Eur. Phys. J. A 20 (2004) 133.
[21] A.P. Zuker, A. Poves, F. Nowacki, S.M. Lenzi, Phys. Rev. C 92 (2015) 024320.
[22] J. Ljungvall, et al., Phys. Rev. C 81 (2010) 061301(R).
[23] S.M. Lenzi, F. Nowacki, A. Poves, K. Sieja, Phys. Rev. C 82 (2010) 054301.
[24] A.P. Zuker, J. Retamosa, A. Poves, E. Caurier, Phys. Rev. C 52 (1995) R1741.
[25] Y. Sun, Phys. Scr. 91 (2016) 043005.
[26] K. Hara, Y. Sun, Int. J. Mod. Phys. E 4 (1995) 637.
[27] J.A. Sheikh, K. Hara, Phys. Rev. Lett. 82 (1999) 3968.
[28] T. Otsuka, M. Honma, T. Mizusaki, N. Shimizu, Y. Utsuno, Prog. Part. Nucl. Phys. 47 (2001) 319.
[29] N. Shimizu, T. Abe, M. Honma, T. Otsuka, T. Togashi, Y. Tsunoda, Y. Utsuno, T. Yoshida, Phys. Scr. 92 (2017) 063001.
[30] N. Shimizu, et al., Prog. Theor. Exp. Phys. 2012 (2012) 01A205.
[31] N. Shimizu, HFB+gcm code, unpublished, 2019.
[32] T.R. Rodriguez, J.L. Egido, Phys. Rev. Lett. 99 (2007) 062501.
[33] B. Bally, A.S. Fernandez, T. Rodriguez, Phys. Rev. C 100 (2019) 044308.
[34] K. Kaneko, Y. Sun, G. de Angelis, Nucl. Phys. A 957 (2017) 144.
[35] K. Kaneko, T. Mizusaki, Y. Sun, S. Tazaki, Phys. Rev. C 92 (2015) 044331.
[36] M. Dufour, A.P. Zuker, Phys. Rev. C 54 (1996) 1641.
[37] T. Otsuka, T. Suzuki, M. Honma, Y. Utsuno, N. Tsunoda, K. Tsukiyama, M. Hjorth-Jensen, Phys. Rev. Lett. 104 (2010) 012501.
[38] K. Kaneko, T. Mizusaki, Y. Sun, S. Tazaki, Phys. Rev. C 89 (2014) 011302(R).
[39] K. Kaneko, N. Shimizu, T. Mizusaki, Y. Sun, Phys. Rev. C 103 (2021) L021301.
[40] D.H. Gloeckner, R.D. Lawson, Phys. Lett. B 53 (1974) 313.
[41] M. Honma, T. Otsuka, T. Mizusaki, M. Hjorth-Jensen, Phys. Rev. C 80 (2009) 064323.
[42] P. Möller, J.R. Nix, W.D. Myers, W.J. Swiatecki, At. Data Nucl. Data Tables 59 (1995) 185.
[43] P. Moller, J.R. Nix, Nucl. Phys. A 361 (1981) 117.
[44] W. Nazarewicz, et al., Nucl. Phys. A 503 (1989) 285.
[45] K. Kaneko, T. Mizusaki, Y. Sun, S. Tazaki, G.de. Angelis, Phys. Rev. Lett. 109 (2012) 092504.
[46] B. Cederwall, et al., Phys. Rev. Lett. 124 (2020) 062501.